

AD-766 213

CENTER FOR HIGH ENERGY FORMING

Henry E. Otto

Denver Research Institute

Prepared for:

Army Materials and Mechanics Research Center

July 1973

DISTRIBUTED BY:

NTIS

National Technical Information Service
U. S. DEPARTMENT OF COMMERCE
5285 Port Royal Road, Springfield Va. 22151



AD

AD 766213

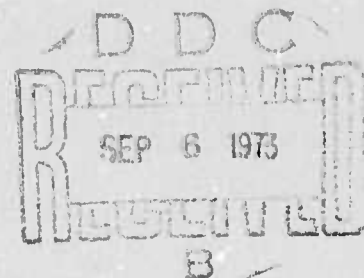
AMMRC CTR 73-23

Center for High Energy Forming

July 1973

Henry E. Otto
Denver Research Institute
University of Denver
Denver, Colorado 80210
(303) 753-2621

Reproduced by
NATIONAL TECHNICAL
INFORMATION SERVICE
U S Department of Commerce
Springfield VA 22151



Second Semi-Annual Technical Report Contract Number DAAG 46-72-C-0130

Approved for public release; distribution unlimited.

Sponsored by
Advanced Research Projects Agency
ARPA Order No. 720

Prepared for

ARMY MATERIALS AND MECHANICS RESEARCH CENTER
Watertown, Massachusetts 02172

| | |
|---------------------------------|--------------------------|
| ACCESSION BY | |
| RTIS | <input type="checkbox"/> |
| B.G. | <input type="checkbox"/> |
| USA | <input type="checkbox"/> |
| JUL 11 1962 | |
| BY | |
| DISTRIBUTION/AVAILABILITY CODES | |
| DISTR. AVAIL. CODE/SPECIAL | |
| A | |

The views and conclusions contained in this document are those of the authors and should not be interpreted as necessarily representing the official policies, either expressed or implied, of the Advanced Research Projects Agency or the U. S. Government.

Mention of any trade names or manufacturers in this report shall not be construed as advertising nor as an official indorsement or approval of such products or companies by the United States Government.

DISPOSITION INSTRUCTIONS

Destroy this report when it is no longer needed.
Do not return it to the originator.

AMMRC CTR 73-23

Center for High Energy Forming

Technical Report by
Henry E. Otto
Denver Research Institute
University of Denver
Denver, Colorado 80210

July 1973

Second Semi-Annual Technical Report Contract Number DAAG 46-72-C-0130

ARPA Order No. 720

Program Code 61101D

Agency Accession Number DA OD 4804

Approved for public release; distribution unlimited.

Prepared for

ARMY MATERIALS AND MECHANICS RESEARCH CENTER
Watertown, Massachusetts 02172

1a

UNCLASSIFIED

Security Classification

DOCUMENT CONTROL DATA - R & D

(Security classification of title, body of abstract and indexing annotation must be entered when the overall report is classified)

| | | |
|---|---|---|
| 1. ORIGINATING ACTIVITY (Corporate author) Denver Research Institute University of Denver | | 2a. REPORT SECURITY CLASSIFICATION UNCLASSIFIED |
| 3. REPORT TITLE Center for High Energy Forming | | 2b. GROUP Details of illustrations in this document may be better studied on microfiche. |
| 4. DESCRIPTIVE NOTES (Type of report and inclusive dates) Second Semi-Annual Report, January 1, 1973 - June 30, 1973 | | |
| 5. AUTHOR(S) (First name, middle initial, last name) Henry E. Otto | | |
| 6. REPORT DATE July 1973 | 7a. TOTAL NO. OF PAGES 2332 | 7b. NO. OF REFS 3 |
| 8a. CONTRACT OR GRANT NO. DAAG 46-72-C-0130 | 8b. ORIGINATOR'S REPORT NUMBER(S) AMMRC CTR 73-23 | |
| b. PROJECT NO. ARPA Order No. 720, Amended | 9b. OTHER REPORT NO(S) (Any other numbers that may be assigned this report) | |
| c. Program Code 61101D | | |
| d. Agency Accession No. DA OD 4804 | | |
| 10. DISTRIBUTION STATEMENT Approved for public release; distribution unlimited. | | |
| 11. SUPPLEMENTARY NOTES Part | 12. SPONSORING MILITARY ACTIVITY Army Materials, Mechanics Research Center Watertown, Massachusetts 02172 | |
| 13. ABSTRACT Studies at the Center for High Energy Forming include: a. A metallurgical Investigation of Explosion Welded Copper-Nickel Composites; b. Determination of the Optimum Parameters for Explosion Welding A515 Steel; c. Analysis and Design of an Explosion Cladding Facility; d. Free Forming Steel Domes with D/t Ratios of 56 and Greater; e. The Mechanics of Energy Transfer from Underwater Explosions; f. The Explosive Free-Forming of Arbitrary Shapes from Thin Metal Sheets; g. Stress Corrosion Cracking Behavior of Explosively Deformed Austenitic Stainless Steel; h. Explosive Thermomechanical Processing of Beta III Titanium Alloy; i. Explosive Compaction of Nickel Base Superalloy Powders; j. Engineering Economics of the Explosive Forming Manufacturing Facilities. | | |

DD FORM 1473

REPLACES DD FORM 1473, 1 JAN 66, WHICH IS OBSOLETE FOR ARMY USE

UNCLASSIFIED

Security Classification

12

Security Classification

Energy Requirements
Energy Transfer
Explosive Welding
Strain Rate Effects
Explosive Powder Compaction
Explosive Forming

Security Classification

ic

FOREWORD

This report covers work done in the period January 1 to December 31, 1973, under the general title *Center for High Energy Forming - Second Semi-Annual Technical Report*. The work is sponsored by the Advanced Research Projects Agency under ARPA Order No. 720, Program Code No. 61101D. The work was sponsored by Army Materials and Mechanics Research Center, Watertown, Massachusetts, 02172, and was monitored by Arthur F. Jones under Contract No. DAAG46-72-C-0130.

ABSTRACT

This report summarizes the results during the period 1 January through June 30, 1973. Studies were conducted in the following areas:

- a. A Metallurgical Investigation of Explosion Welded Copper-Nickel Composites;
- b. Determination of the Optimum Parameters for Explosion Welding A515 Steel;
- c. Analysis and Design of an Explosion Cladding Facility;
- d. Free Forming Steel Domes with D/t Ratios of 56 and Greater;
- e. The Mechanics of Energy Transfer from Underwater Explosions;
- f. The Explosive Free-Forming of Arbitrary Shapes from Thin Metal Sheets;
- g. Stress Corrosion Cracking Behavior of Explosively Deformed Austenitic Stainless Steel;
- h. Explosive Thermomechanical Processing of Beta III Titanium Alloy;
- i. Explosive Compaction of Nickel Base Superalloy Powders;
- j. Engineering Economics of the Explosive Forming Manufacturing Facilities.

CONTENTS

| | <u>Page</u> |
|---|-------------|
| Foreword. | i |
| Abstract. | .iii |
| Contents. | v |
| 1. A Metallurgical Investigation of Explosion Welded Copper-Nickel Composites. | 1 |
| 2. Determination of the Optimum Parameters for Explosion Welding A515 Steel. | 4 |
| 3. Analysis and Design of an Explosion Cladding Facility | 7 |
| 4. Free Forming Steel Domes with D/t Ratios of 56 and Greater. | 8 |
| 5. The Mechanics of Energy Transfer from Underwater Explosives | 10 |
| 6. The Explosive Free-Forming of Arbitrary Shapes from Thin Metal Sheets | 11 |
| 7. Stress Corrosion Cracking Behavior of Explosively Deformed Austenitic Stainless Steels. | 12 |
| 8. Explosive Thermomechanical Processing of Beta III Titanium Alloy. | 15 |
| 9. Explosive Compaction of Nickel Base Superalloy Powders. | 21 |
| 10. Engineering Economics of Explosive Forming Manu- facturing Facilities. | 23 |
| Figures | |
| 1. Boltzman - Mantano Diffusion Coefficient for Copper as a Function of Temperature in Copper-Nickel Systems. | 3 |
| 2. Typical Strain Curve for Explosively Free-Formed AISI 310 Dome. | 13 |
| 3. Photomicrograph of Surface of Beta III Titanium Strained at $2.25 \times 10^{-5} \text{ sec}^{-1}$ | 17 |
| 4. Photomicrograph of Surface of Beta III Titanium Strained at $2.25 \times 10^{-3} \text{ sec}^{-1}$ | 17 |
| 5. Photomicrograph of Surface of Beta III Strained at $2.25 \times 10^{-1} \text{ sec}^{-1}$ | 18 |
| 6. Photomicrograph of Section Parallel to Surface of Specimen Strained at $2.25 \times 10^{-5} \text{ sec}^{-1}$ | 18 |

| | <u>Page</u> |
|---|-------------|
| 7. Photomicrograph of Section Parallel to Surface of Specimen Strained at $2.25 \times 10^{-3} \text{ sec}^{-1}$ | 19 |
| 8. Photomicrograph of Section Parallel to Surface of Specimen Strained at $2.25 \times 10^{-1} \text{ sec}^{-1}$ | 19 |
| 9. Photomicrograph of Explosively Formed Beta III Titanium. | 20 |
| 10. Photomicrograph of Beta III Titanium Shocked at 317 kbars. | 20 |
| 11. Schematic Sketch of Hot Explosive Compaction Assembly. | 22 |

Table

| | |
|---|---|
| 1 Concentration Dependence of Diffusivity for Cu-Ni Loaded 8g/sq in 40% Red Cross Dynamite | 2 |
|---|---|

1. A Metallurgical Investigation of Explosion Welded Copper-Nickel Composites.

Faculty Advisors: S.H. Carpenter and H.E. Otto

Graduate Student: M.D. Nagarkar

Further work was carried out in the analysis of diffusion data on explosion welded and roll-bonded copper-nickel composites. As reported earlier, roll-bonded Cu-Ni couples were explosion welded to each other to form Ni-Cu-Ni-Cu composites. These and the pure roll-bonded specimens were subsequently heat-treated for 10 hours in vacuum at annealing temperatures of 500, 750, 900, and 975°C. To determine the extent of diffusion across each interface the electron microprobe method of analysis was used. A computer program, as described by Brown¹ was used for calculating the composition of Copper in atomic percent from the measured X-ray data. This program corrects the measured X-ray intensities to relative intensities and also applies necessary corrections to the latter for absorption, secondary fluorescence, and atomic number effects.

Plots of concentration versus diffusion width had indicated enhanced diffusion across the interface of the explosion weld as compared to the pure roll-bonded interface as well as the Cu-Ni interface of the cladder plate and of the base plate. For a more meaningful analysis of the diffusion data, it was necessary to determine the diffusion coefficients (D). In Cu-Ni D is concentration-dependent, hence the Boltzman-Matano method of determination of D was found most suitable.

For greater accuracy and speed, a computer program was written to carry out the Boltzman-Matano analysis. This program yields values of D at different concentrations of Cu across the interface. A typical result obtained from the computer is given in Table 1.

The data at present analyzed is of Cu-Ni weld using an explosive loading of 8 g/sq. in. At annealing temperatures above 750°C, diffusion was found to follow an Arrhenius type of relation:

$$D = D_0 e^{\frac{-Q}{RT}}$$

where D is the Diffusion Coefficient,

D_0 , the frequency factor which is independent of the annealing temperature,

Q, the activation energy, R the gas constant, and

T, the annealing temperature in degrees Kelvin.

1. J.D. Brown, 'Comprehensive Computer Program for Electron Probe Microanalysis', Anal. Chem., 38, No. 7, 890 (1966)
2. B. Ya. Pines, I.G. Ivanov and I.V. Smushkov, Soviet Physics.-Solid State, 4, 7, 1380 (1963).

The plot D vs. $1/T$ yields a straight line, and from the slope the activation energy can be calculated. Figure 1 shows a D vs. $1/T$ plot for Cu-Ni at 8 g/sq. in. explosive loading. Similar analysis is being done for welds made at a higher explosive loading, viz. 12 g/sq. in.

Table 1. Concentration dependence of diffusivity for Cu-Ni loaded 8 g/sq.in. 40% Red Cross Dynamite (Traverse across crest of wavy explosion welded interface)

| Temperature (°C) | Time of anneal (sec) | Concentration of Copper (Atomic %) | Diffusion Coefficients (cm ² /sec) |
|---------------------|----------------------------|---------------------------------------|---|
| 975 | 36×10^3 | 90 | 1.85×10^{-10} |
| | | 85 | 1.44×10^{-10} |
| | | 80 | 7.53×10^{-11} |
| | | 75 | 4.91×10^{-11} |
| | | 70 | 3.65×10^{-11} |
| | | 65 | 2.90×10^{-11} |
| | | 60 | 2.38×10^{-11} |
| | | 55 | 1.99×10^{-11} |
| | | 50 | 1.68×10^{-11} |
| | | 45 | 1.42×10^{-11} |
| | | 40 | 1.20×10^{-11} |
| | | 35 | 1.00×10^{-11} |
| | | 30 | 8.33×10^{-12} |
| | | 25 | 6.75×10^{-12} |
| | | 20 | 5.29×10^{-12} |

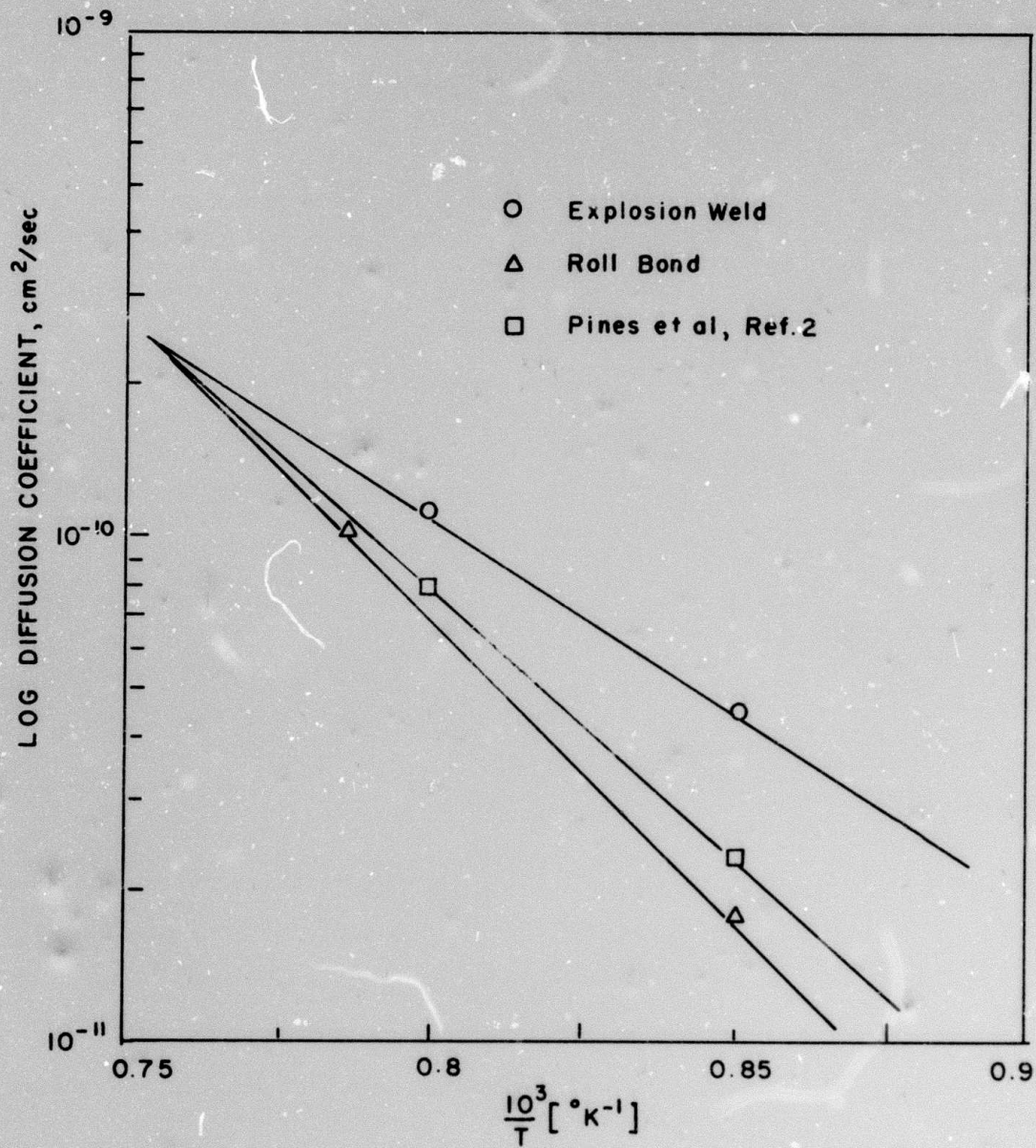


Figure 1. Boltzman - Mantano Diffusion Coefficient for Copper as a Function of Temperature in Copper-Nickel Systems

2. Determination of the Optimum Welding Parameters for Explosion Welding A515 Steel

Faculty Advisor: H. Otto

Graduate Student: Steven Stivers

Explosives with lower detonation velocities than used previously were used to weld the A515 steel to improve the wave formation at the interface. Initial tests were conducted using DePont Red Crown 70% dynamite. This explosive has a higher detonation velocity than the 40% Red Cross Extra that was originally scheduled to be used but DuPont has discontinued production of the Red Cross Extra. The tests with 70% Red Crown dynamite had an improved wave structure but were still lacking in overall quality.

An analytical approach was then taken to correlate the empirical welds with surface wave phenomena. The analytical approach was based upon several observations and facts. First, the characteristic waves formed during explosion bonding are confined to an area near the interface and the motion damps out rapidly as the distance from the interface increases. Second, the sonic velocity of the material being welded has been shown to be an important parameter. The sonic velocity has been defined as $C = \frac{\rho}{\mu}$ where ρ is the density and μ is an elastic constant. Third, the sonic velocity varies from metal to metal as does the characteristic amplitude and frequency of the explosion bonds with different metals.

Rayleigh surface waves describe systems where an isotropic solid has a bounding surface. They decrease rapidly with depth and the velocity is less than that of a body wave. Another criteria is that the boundary is stress free; i.e. the principal stress components σ_{zz} , σ_{zy} and σ_{zx} vanish at the surface. Rayleigh waves are derived from the equations of motion of an isotropic solid in which body forces are absent. If the free boundary is the xy plane with the z positive axis orientated towards the interior and the direction of motion is along x, the equation of motion for an isotropic elastic media is:

$$\rho \frac{\partial^2}{\partial t^2} (u, v, w) = (\lambda + \mu) \left(\frac{\partial \Delta}{\partial x}, \frac{\partial \Delta}{\partial y}, \frac{\partial \Delta}{\partial z} \right) + \mu \nabla^2 (u, v, w)$$

Since the wave motion will be independent of the y direction, two potential functions ϕ , ψ can be defined such that

$$u = \frac{\partial \phi}{\partial x} + \frac{\partial \psi}{\partial z} \quad \& \quad w = \frac{\partial \phi}{\partial z} - \frac{\partial \psi}{\partial x}$$

When the potential functions are substituted,

$$\rho \frac{\partial}{\partial x} \left(\frac{\partial^2 \phi}{\partial t^2} \right) + \rho \frac{\partial}{\partial z} \left(\frac{\partial^2 \psi}{\partial t^2} \right) = (\lambda + 2\mu) \frac{\partial}{\partial x} (\nabla^2 \phi) + \mu \frac{\partial}{\partial z} (\nabla^2 \psi)$$

$$\& \quad \rho \frac{\partial}{\partial z} \left(\frac{\partial^2 \phi}{\partial t^2} \right) - \rho \frac{\partial}{\partial x} \left(\frac{\partial^2 \psi}{\partial t^2} \right) = (\lambda + 2\mu) \frac{\partial}{\partial t} (\nabla^2 \phi) - \mu \frac{\partial}{\partial x} (\nabla^2 \psi)$$

These two equations will be satisfied if:

$$\frac{\partial^2 \phi}{\partial t^2} = [(\lambda + 2\mu/\rho)] \nabla^2 \phi = c_1^2 \nabla^2 \phi$$

$$\frac{\partial^2 \psi}{\partial t^2} = [\mu/\rho] \nabla^2 \psi = c_2^2 \nabla^2 \psi$$

The first equation representing dilatational waves and the second, distortion waves. These equations have the same form as the equation describing a vibrating membrane and the solutions are:

$$\phi = f(z) \exp [i (\rho t - fx)]$$

$$\psi = g(z) \exp [i (\rho t - fx)]$$

where $f(z)$ and $g(z)$ describe the way in which amplitude of the waves vary with z . To determine the relationship, substitute ϕ & ψ into the "membrane" equation. The resulting equations

$$\phi = A \exp[-qz + i(\rho t - fx)]$$

$$\psi = B \exp[-st + i(\rho t - fx)]$$

show the exponential decay of the z direction wave. Further manipulation and substitution of the boundary conditions give rise to a cubic equation in K^2 where K is the ratio of distortion to surface wave velocity. Using Poisson's ratio a numerical solution can be obtained. Solving the cubic equation for various materials gives a comparison of theory and experimental values. Results of this comparison is presented below:

| <u>Metal</u> | <u>Theoretical</u> | <u>Experimental</u> |
|--------------|--------------------|---------------------|
| Copper | 1965 m/sec | - |
| Aluminum | 2780 m/sec | 2500-2800 m/sec |
| Nickel | 3057 m/sec | 3000-3250 m/sec |
| Steel | 2939 m/sec | 2300 - N.D. |

This approach does give velocities for wave formation that is consistent with experimental results. Shortcomings of this approach are (1) it does not give a range of velocities over which waves can form (2) it does not predict the variations in amplitude and (3) the correlation is due more to the closeness of wave and sonic velocity rather than being a unique function of the wave phenomena.

Experiments were conducted with 40% free running dynamite ($V_D = 2200$ m/sec in amount used). These tests not only gave good wave formation but excellent strengths. Tensile strengths ranged from 60,000 to 104,000 psi compared with a base metal strength of 77,000 psi. Wave patterns were well defined with little or no melt at the interface. Further tests were conducted to ascertain if the collosion point velocity was the primary factor in the improved welds obtained with the 40% free running dynamite. The tests were conducted with 70% Red Crown and a preset angle whereas those with a free running were of the parallel configuration. In the preset angle weld the collosion point velocity is related to the explosive detonation velocity by the relationship:

$$V_c = V_d \frac{\sin \beta}{\sin (\alpha + \beta)}$$

where: V_c = collosion point velocity

V_d = detonation velocity

α = preset angle

β = dynamic bend angle

It is possible to lower the collosion point velocity by changing the preset angle. These tests indicated that the wave formation was related to the collosion point velocity.

The successful welds were then compared with a second model based on the fact that the wave formation is turbulent above a characteristic Reynolds number. For this comparison it is important to obtain accurate measurements of the detonation and collosion point velocities. This was done by using a technique used by Ribovich et. (1) and adapted by Wittman(2) for measuring the collosion point and explosive detonation velocities. Comparisons using this model based on hydronamic models has met with a high degree of initial success.

Effort is now being placed on further refinement of the model and to relate the Reynolds number for transition to dynamic welding parameter.

1. J. Ribovich, R. Watson and F. Gibson, Instrumental Card-Gap Test, AIAA Journal, 6 #7, 1968.
2. R.H. Wittman, Unpublished Data.

3. Analysis and Design of an Explosion Cladding Facility

Faculty Advisor: A. Ezra

Graduate Student: A. Eriksen

An explosive cladding facility has been designed as a shell structure to cover the charge and the immediate work area in order to reduce blast pressure to personnel and equipment.

A hemispherical shell of mild steel was found to be the most feasible structure to resist internal blast loading. The diameter of the shell was determined to be 20 feet and the thickness 1 inch. The stress level in the shell under repeated loads will be elastic to meet the purpose of design. The use of mild steel for the shell will insure sufficient ductility to avoid failure if localized stresses become excessive. To decrease the blast pressure it was decided that a certain degree of vacuum maintained during the explosion would be advantageous.

The behavior of this structure exposed to a blast wave may be considered under two main headings. The first is called the "loading," i.e., the magnitude and duration of the blast pressure. The other is the response of the structure due to the blast loading. There are numerous factors associated with the characteristics of a structure which influence the response to the blast wave accompanying an explosion. The most important include the modulus of elasticity, stiffness, mass of the structure and structural shape.

A theoretical analysis based on the membrane theory was developed and appears to give a good approximation of the stresses in the shell as long as the ratio of the shell radius to the shell thickness is large. Where bending stresses do occur, they will be localized in nature, occurring primarily near the base.

Verification of the calculations of hoop stresses based on some simplifying assumptions was attempted by testing. The most efficient way to do this was to use a small scale model. The model used was 1/20th scale, having a diameter of 12 inches and a thickness of 0.05 inches. The model hemispherical dome was formed using explosive forming. It is assumed that this method is also applicable for the prototype. The dynamic strain measurements on the scale model were carried out using strain gages attached to the surface of the dome. Tests were only partially successful and further testing is planned.

4. Free Forming Steel Domes with D/t Ratios of 56 and Greater

Faculty Advisor: E. Wittrock

Graduate Student: J. Freeman

Work was continued on free forming steel domes with D/t ratios of 56 and greater. As reported in the Semi-Annual Technical Report (DAAG46-72-C-0130, January 1973) steel blanks with D/t ratios of 28 had been free formed into domes which were relatively free of edge wrinkles and had a smooth surface finish. Subsequently, as a part of the present program, it was decided to determine if the D/t ratio could be increased, with similar results. Two thicknesses of mild steel plate were used in these tests, i.e., 1/4 inch and 1/8 inch. Both thicknesses were cut into circular blanks 14 inches in diameter.

Testing was initiated using the 1/4 inch thick blanks of A-36 steel. (D/t = 56) using the setup patterned after the original tests on the 1/2 inch thick blanks. It was determined that a pancake charge measuring 6.0 inches in diameter by 0.25 inches thick and containing 110 grams of SWP-5 would form these blanks to an initial draw depth which was considered to be close to the optimum. However, due to the thickness of the blanks, the edge wrinkles were always very deep. (The depth of the edge wrinkles can be characterized by the bend angle. Thus a very shallow wrinkle would have a bend angle of, say, 10° to 20°. A very deep wrinkle would show the material bent about 180° with a very small bend diameter.)

Consequently, as pointed out in the previous report, the domes would not respond to the spherical sizing shot since the energy required to straighten the wrinkles far exceeded that which would blow out the center of the domes. In an effort to distribute the energy more efficiently to the wrinkled portions of the domes, the sizing shot geometry was changed to a pancake shape which placed the periphery of the charge out near the wrinkles. As of the last reporting period, a pancake charge 5.3 inches in diameter by 0.35 inches thick containing 135 grams of SWP-6 had been fired in these domes without making significant changes in the shape.

The effort to free form and size the 1/4 inch thick blanks was continued to determine if the initial shape due to the forming shot could be changed in such a way that the sizing shot would be more effective. Basically, the forming shots were changed so that the initial shape of the dome was a shallow pan with the steep sides. This change made the wrinkles shallower and shorter, i.e., the wrinkled material did not extend as far in towards the center of the dome. This change in shape of the domes was accomplished primarily by increasing the diameter of the void or airspace from 10 inches to 12 inches, and by introducing a standoff (air space) between the sides of the pancake charge and the blanks. In some cases only the diameter of

the void was changed. When sizing shots were fired in these domes, the results were essentially the same as those found previously. That is, either the charge was too light and no significant sizing was observed, or the charge was too heavy in which case the center of the dome was cracked or blown out. This was true regardless of the sizing charge geometry (spherical or pancake). In no instance was there any meaningful improvement in the shape of the domes or in the size of the wrinkles. During this same period four shots were fired using 14 inch diameter by 1/8 inch thick blanks for a D/t ratio of 113. Results of these tests verified that the effect of the high D/t ratio is to increase the wrinkle length and depth during the forming shot, making the sizing and wrinkle straightening even more difficult. In the case of the 1/8 inch thick blanks the wrinkles would usually be deep enough that the bend angle was near 180°.

Based on the foregoing, it must be concluded that free forming thin steel blanks with D/t ratios greater than about 36 (18 inches diameter by 1/2 inch thick) the edge wrinkles will be too deep to permit explosive sizing of the domes. It is possible that other methods of explosive forming could be applied to this problem, such as firing numerous small charges thereby forming the domes in small increments, but no such program is planned or anticipated at this time.

5. The Mechanics of Energy Transfer from Underwater Explosions

Faculty Advisor: G. Thurston

Graduate Student: V. D'Souza

The explosive forming of domes without a die requires a prediction of the final deformations and strain distribution in the dome for various charge strengths and standoff distances as well as various plate sizes and material properties. This prediction is useful when a sizing die is used to give the final shape. Die life can be increased and springback reduced in sizing if the nearly formed shape hits the die with a low velocity.

While the initial loading due to the shockwave from the explosion has been reasonably well predicted and correlated with experiments, the later complex loading on the plate termed the reloading phenomenon, has obstructed the goal of prediction of the final shape and strains in the dome.

In this study a model of the reloading phenomenon is used which would predict the final deformations and strains of a plate acted upon by an underwater explosion. The effect on the dome shape and strains, as predicted by this theory, will be evaluated for various charge and plate parameters.

The thin uniform thickness circular blank is held between frictionless annular rings. This set-up is immersed in a sufficient depth of water so that the gas bubble of the explosion products does not vent before the reloading takes place. The charge in the shape of a sphere is placed at an appropriate standoff distance and set off. The resulting motion of the deforming blank is studied analytically and the final strains and shape of the dome that is formed is computed.

The problem can be considered as consisting of two parts - first to determine the pressure loading on the blank as a function of time and secondly to use this pressure in computing the dynamic response of the blank during the large plastic deformations that occur. Both these aspects of the problem are coupled and hence a computer solution will be sought. The problem is complex because of the various interactions, but by means of suitable approximations that represent the physical phenomenon, a realistic model that provides good correlation with experiments is expected.

6. The Explosive Free-Forming of Arbitrary Shapes from Thin Metal Sheets

Faculty Advisor: M. A. Kaplan

Graduate Student: S. Y. Aku

The basic aim of the study is to learn enough about the role of the important parameters in the explosive forming process to enable arbitrary shapes to be formed without the need for extensive trial and error testing. In the first phase of the study, the effects of charge shape, weight, and location are being studied on the deformation of an "infinite" sheet. The infinite sheet is being used so that there will be no influences of the boundaries on the deformation of the workpiece.

Since the last progress report, an analytical model has been formulated for describing the deformation of an infinite thin plate produced by the detonation of a single point charge in air. The model uses an initial plate velocity distribution calculated from acoustic theory. It is assumed that a concentric plastic hinge is initially formed which moves radially inward with time. The plate is assumed to deform by bending during this phase of its motion. After the plastic hinge reaches the center of the plate, further deformation by stretching is assumed. This model predicts the final deformation with a fair degree of accuracy.

The model is now being generalized to handle an arbitrary axially symmetric distribution of charge and a line charge. Some experiments with other than a point charge configuration have been conducted and it has been discovered, that the final deformation can be roughly approximated by superimposing the deformations produced by individual charges. The theory indicates that this is possible under certain conditions.

7. Stress Corrosion Cracking Behavior of Explosively Deformed Austenitic Stainless Steels

Faculty Advisor: H. Otto and R.N. Orava

Graduate Student: Edward Chang

The explosive free forming of AISI 304 and 310 blanks, 0.5 in thick and 22 in diameter, were carried out by a sandwich method using a pancake type charge developed by Alting¹ and refined by Wittrock². The stainless steel domes required 694 grams of Trojan SWP-5 explosive to obtain the desired deformation.

Photo grids with polar coordinates, 8 inch in diameter, were made on the blanks prior to explosive forming. As in prior work, the effective strain, ϵ^* , was calculated using the measured circumferential and radial strains. The domes were not sized so the strains were not symmetrical across the domes. There is no necessity for a uniform strain since the only use of the domes is to provide specimens for testing. A typical effective strain curve is shown in Figure 1. Strains for the AISI 304 domes range from about 11 to 42 percent and those for the AISI 310 from about 12 to 39 percent. There was very little difference in the forming characteristics for the two materials.

The effective strains on the AISI 310 and 304 stainless steel domes ranged from 0.38 at the center to 0.12 at a distance of 7 inches from center.

Comparisons in tensile strength, yield strength and stress corrosion cracking properties will be made among explosively free-formed, cold rolled, and undeformed material. The cold rolling will be carried out by cross rolling to produce a corresponding strain state to that of explosively free-formed.

The stress corrosion cracking test will be performed by a three point bending method with precracked specimens in 3.5% NaCl solution at room temperature. Time to failure at various K_I levels will be measured and the apparent threshold for stress corrosion cracking, K_{Isc} will be determined.

The fractured surfaces will be examined by optical, scanning and transmission electron microscopy to evaluate any structural differences such as martensitic transformation, microcracks, twins, carbide formation and distribution and other physical features.

Part of the comparison of the explosively and conventionally strained materials will be conducted on stress relieved stock. There has been work on explosively formed stock in which the resistance to stress corrosion was reported to have been degraded. Proper adjustment of the

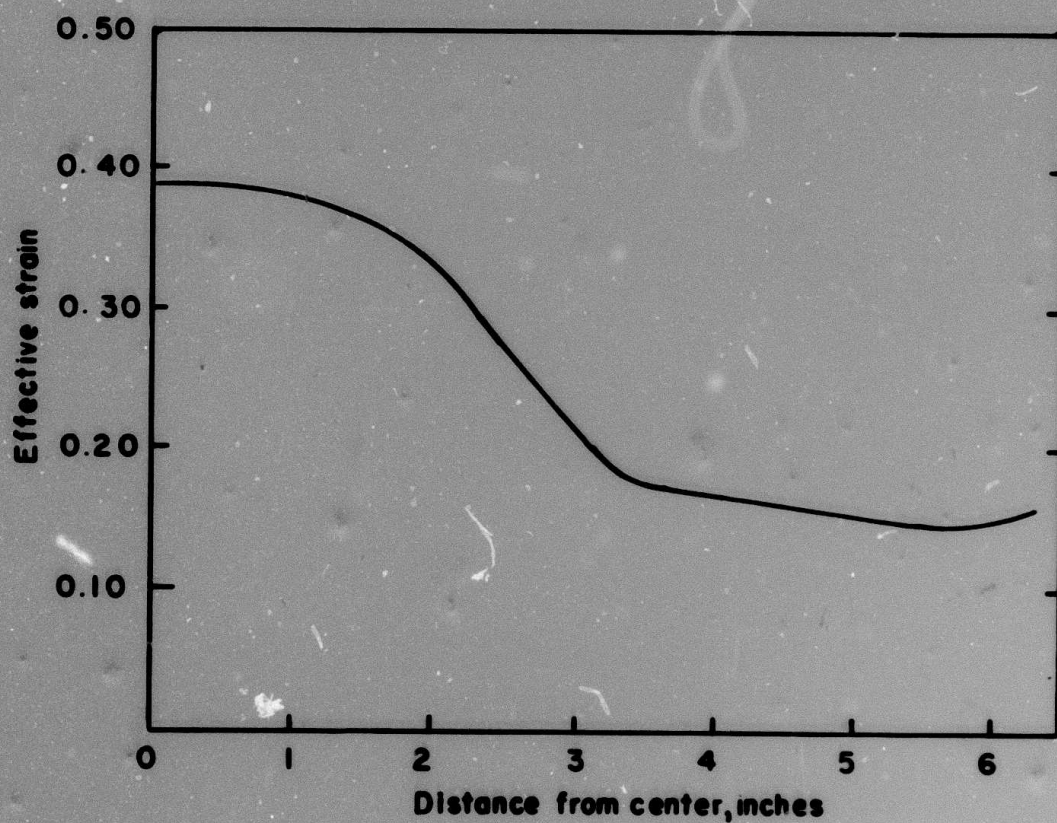


Figure 2 - Typical Strain Curve for Explosively
Free-Formed AISI 310 Dome

stress relief treatment could alleviate this problem, if it occurs.

1. L. Alting, Explosive Forming of Domes, Proceedings Third International Conference of the Center for High Energy Forming, 6.1.1, Vail, Colorado, 1971.
2. E.P. Wittrock "Explosive Forming of Thick Walled Domes", Final Report, DRI #2600, Univ. of Denver, (1972).

8. Explosive Thermomechanical Processing of Beta III Titanium

Faculty Advisor: R.N. Orava

Graduate Student: M.B. de Carvalho

Mechanical property data has been obtained on Beta III titanium both in the conventionally and explosively processed conditions. Correlation of the mechanical properties with metallurgical and crystallographic features is being conducted. For this correlation several tests have been conducted or are in the process of being performed. These include: (a) tensile tests at different strain rates, (b) X-ray diffraction studies, (c) characterization of surface and internal microstructures and (d) pre-straining aging treatments.

(a) Mechanical properties of Beta III Titanium tested at different strain rates

Specimens of as-received stock (solution Treated at 1350°F) were tested using three different strain rates: (1) $2.25 \times 10^{-5} \text{ sec}^{-1}$, (2) $2.25 \times 10^{-3} \text{ sec}^{-1}$, and (3) $2.25 \times 10^{-1} \text{ sec}^{-1}$. These tests were used to determine the work hardening rate and the strain hardening coefficient. The results are as follows.

| <u>Rate</u> | <u>Total Strain, E</u> | <u>Strain Hardening Coefficient, n</u> | <u>Work Hardening rate(K), ksi</u> |
|--|------------------------|--|------------------------------------|
| $2.25 \times 10^{-5} \text{ sec}^{-1}$ | 0.0380 | 0.091 | 250 |
| $2.25 \times 10^{-3} \text{ sec}^{-1}$ | 0.0380 | 0.078 | 212 |
| $2.25 \times 10^{-1} \text{ sec}^{-1}$ | | (1) | (1) |

(1) Rate too high for accurate determination.

The trend in these tests was for the work hardening rate to decrease with increasing strain rates.

Prior to testing, the specimens were chemically polished so the surface could be examined metallographically after straining. Photomicrographs of specimens strained at the different rates are presented in Figures 2 through 4. An inspection of these photomicrographs indicates a difference in surface morphology as a result of strain rate. Several possibilities could explain the difference in surface morphology including (1) the formation of martensite at higher strain rates, (2) the deformation made is a combination of slip and twinning with increasing twinning at higher rates and (3) twinning is the predominant deformation mode. X-ray diffraction studies were conducted to determine the micro structural constituents.

(b) X-ray diffraction studies

Samples in the following conditions were examined (1) As received-

non deformed (2) explosively formed and (3) shocked. The results of this investigation indicated that there was no difference in the constituents. All of the specimens contained the beta (BCC) and omega (HCP) phases. The omega phase, which forms on quenching, was minute in all cases. These results would indicate that martensite does not form at high strain rates.

(c) Metallographic Examinations

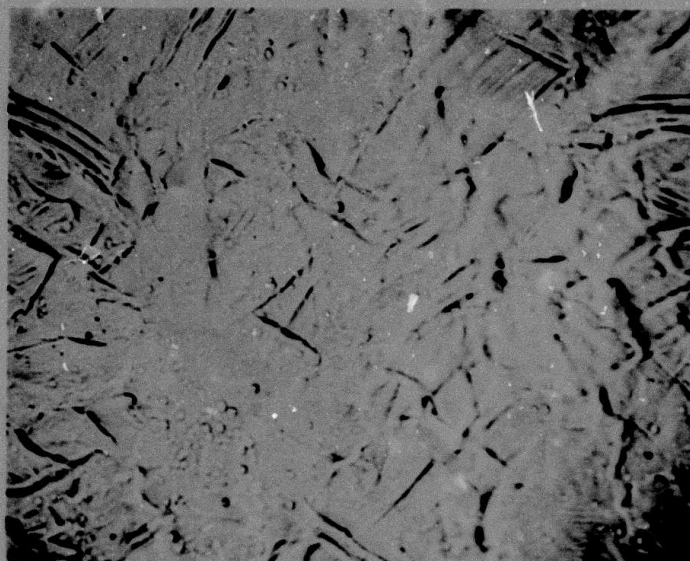
The surface deformation indicated the possibility of slip at lower strain rates and twinning at higher strain rates. The surface of the specimens were ground and polished further to determine if the surface features were slipbands or twins. The markings did not disappear during this procedure which indicated that the deformation mode was twinning. This was true for the materials strained at different rates, explosively formed and shocked. The microstructures of these specimens are shown in Figures 5 to 9.

In comparing these photomicrographs it can be seen that those of the explosively formed and shocked are similar to the one strained at a high strain rate. The lower strength of the explosively formed material can be ascribed to the twinning deformation mode.

(d) Pre-Straining Aging Treatments

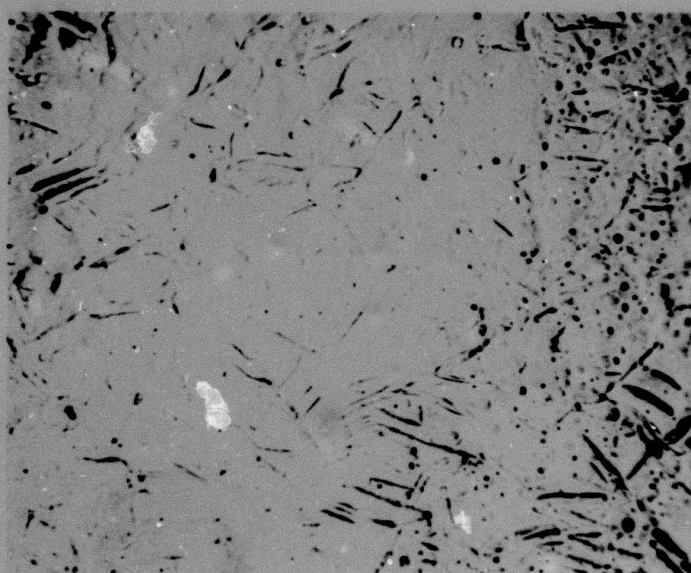
A series of aging treatments were conducted to optimize the hardness prior to deformation. These tests were conducted at 900°F for various periods of time. The hardness increases with increasing time at temperature. The major increase in hardness occurs within the first ten minutes (31 to 39 Rc) after which it increases by only a small amount.

Material aged for 10 minutes will be used in the next series of explosive forming tests.



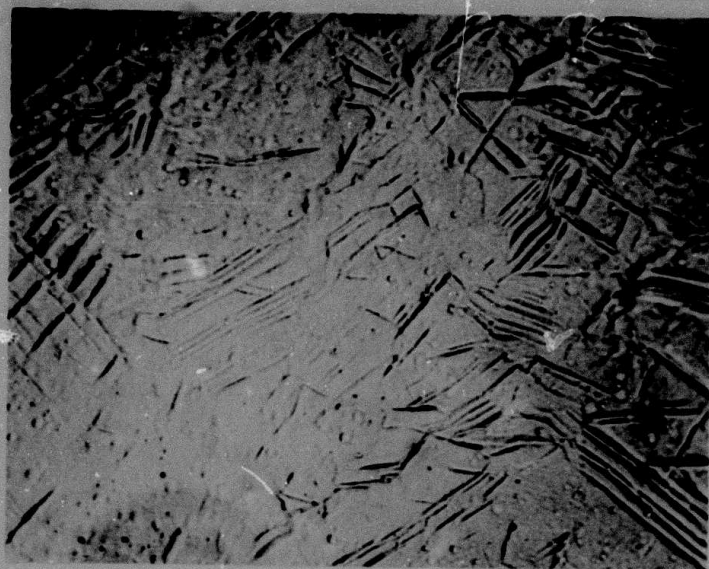
500X

Figure 3. Photomicrograph of Surface of Beta III Titanium
Strained at $2.25 \times 10^{-5} \text{ sec}^{-1}$



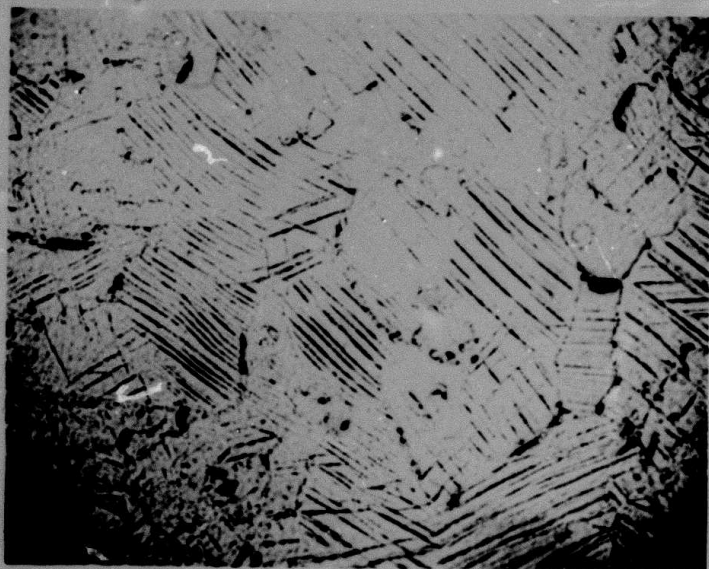
500X

Figure 4. Photomicrograph of Surface of Beta III Titanium
Strained at $2.25 \times 10^{-3} \text{ sec}^{-1}$



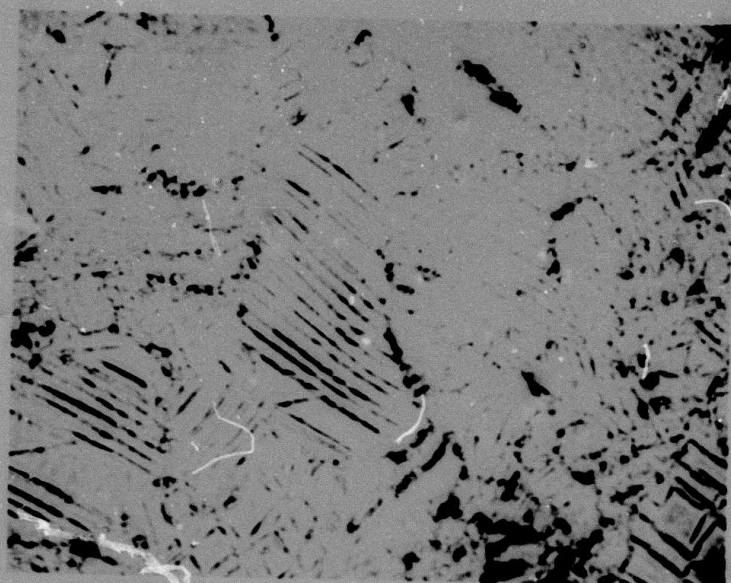
500X

Figure 5. Photomicrograph of Surface of Beta III Strained at $2.25 \times 10^{-1} \text{ sec}^{-1}$



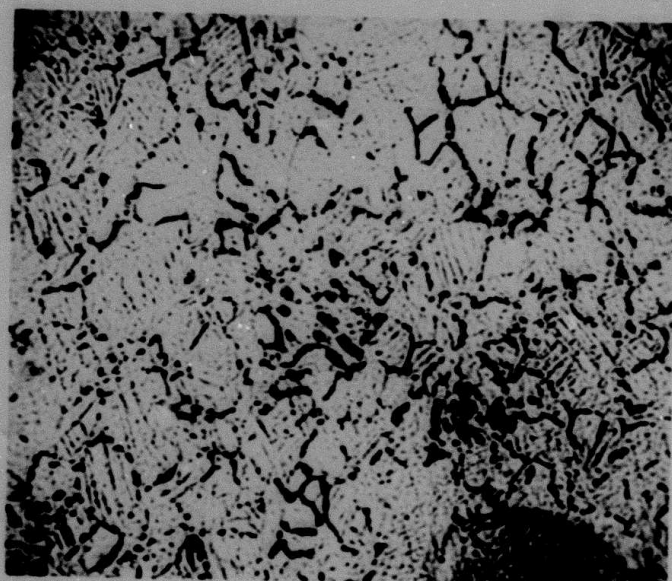
500X

Figure 6. Photomicrograph of Section Parallel to Surface of Specimen Strained at $2.25 \times 10^{-5} \text{ sec}^{-1}$



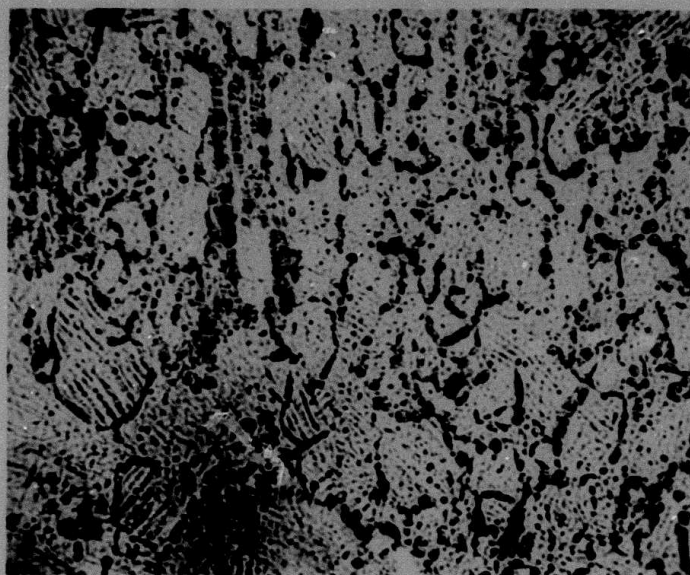
500X

Figure 7 . Photomicrograph of Section Parallel to Surface
of Specimen Strained at $2.25 \times 10^{-3} \text{ sec}^{-1}$



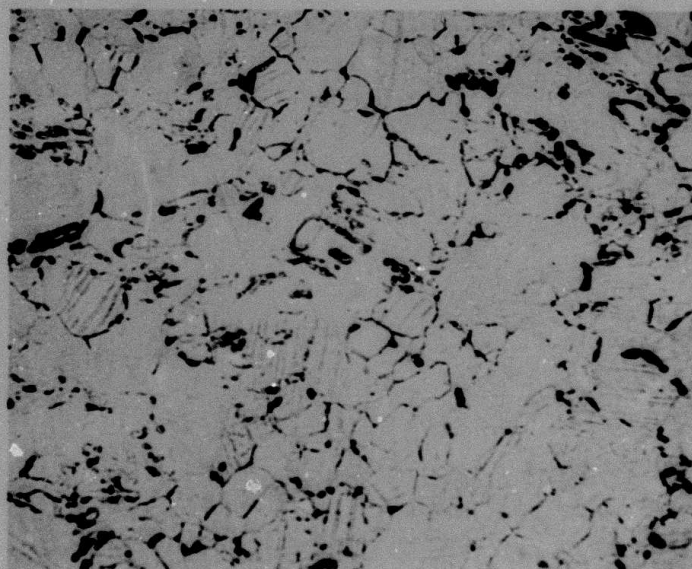
500X

Figure 8 . Photomicrograph of Section Parallel to Surface
of Specimen Strained at $2.25 \times 10^{-1} \text{ sec}^{-1}$



500X

Figure 9. Photomicrograph of Explosively Formed
Beta III Titanium



500X

Figure 10. Photomicrograph of Beta III Titanium
Shocked at 317 kbars

9. Explosive Compaction of Nickel Base Superalloys

Faculty Advisor: H. Otto

Graduate Student: T. McClelland

Emphasis has been placed during the past few months on developing a technique to hot explosively compact metal powders. Cold explosive compaction of Udimet 700 powder indicated that cracks in the compact could be anticipated using a tubular implosion technique. A method has been developed to explosively hot compact metal powders. Safety was one of the primary considerations since the explosive used (dynamite) is heat sensitive.

A schematic sketch of the explosive compaction assembly is shown in Figure 10. The evacuated tube holding the metal powder is heated first to the compaction temperature. This tube is then placed in an insulated transfer container to take it to the blast site. The compaction assembly consists of a drop tube to guide the powder container to the explosive. The explosive charge rests on a glass plate over a barrel of water. A blast triggering switch is on top of the glass so when the container hits the switch the blast is set off.

A pin is inserted through the drop tube at the top to hold the powder container and prevent dropping while personnel are close by. This pin is pulled out with a rope leading to the personnel bunker. Glass was used to hold the dynamite and triggering switch so if the triggering switch did not work, the hot powder container would break through the glass into the water. This feature prevents arrest of the powder container in the center of the explosive charge which could be set off by the heat. Also, in regular use the water quenches the compact immediately after compaction.

The assembly has been tested for both cold and hot compaction. Ancorsteel 1000 iron powder was used during the trial runs. The heat loss during transfer from the furnace to the blast site has been determined to be less than 100°F. Hot compaction of the iron powder at 1600°F has resulted in compacts with densities in excess of 95 percent of theoretical.

The next step will be the compaction of the nickel-base superalloy, René 95. This powder is being supplied by the Carpenter Technology Corporation.

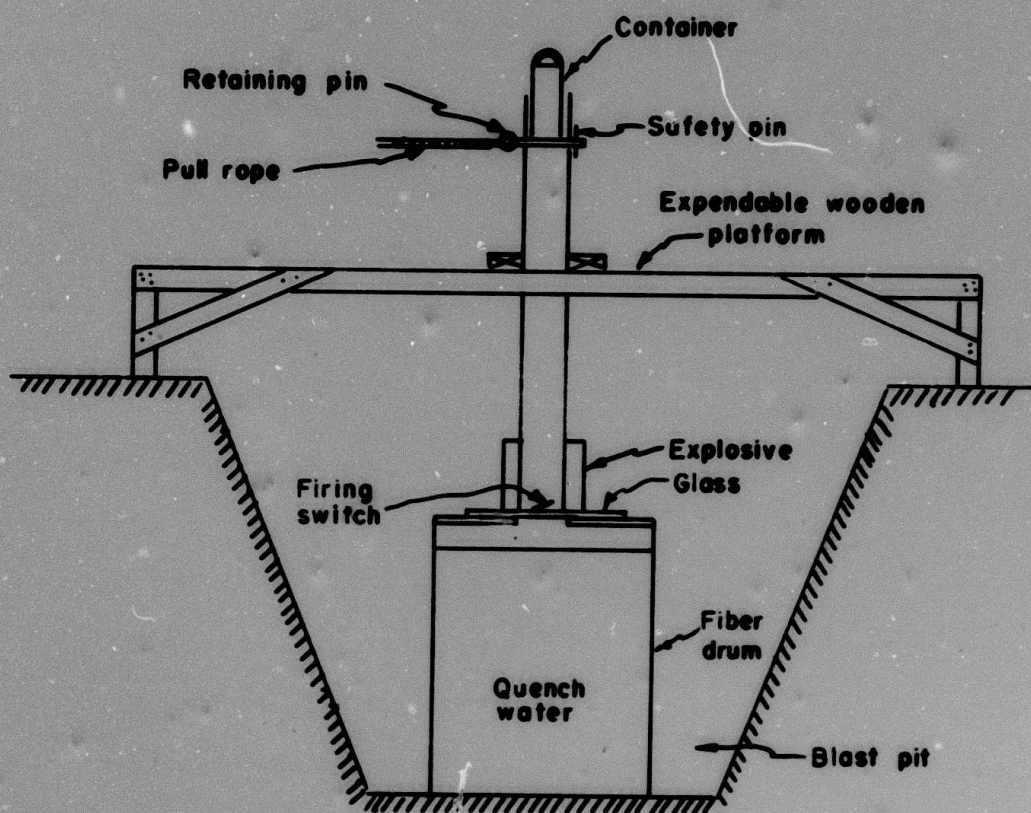


Figure 11. Schematic Sketch of Hot Explosive Compaction Assembly

10. Engineering Economics of the Explosive Forming Manufacturing Facilities

Faculty Advisor: Gordon Milliken

Graduate Student: Arvind P. Teotia

Aside from the several technological advantages of the explosive forming process that give it a role in industry today, there is a significant economic advantage. A big capital investment is largely eliminated, as expensive machinery is not needed. The object of this study is to analyze and evaluate the capital investment required for several different sizes of facilities for production forming of A. S. M. E. Flanged and Dished heads. Such evaluation will permit the economics of explosive forming technique to be compared with the alternative manufacturing process.

In the first part of the study, the explosive forming pool requirements are analyzed. A steel-lined tank, located below ground, is found to be the most suitable facility. For the different quantities of TNT explosive, the tank dimensions are designed taking into consideration the type of soil and the presence of a concrete wall apron around the tank. The pre-design estimates of the construction and installation cost of these cylindrical mild steel fabricated tank facilities are evaluated.

Secondly, the several supporting facilities in the form of air and vacuum system, heating and filter equipment, material handling system and various utilities are designed for different forming facilities and costs are subsequently estimated.

The total cost of the main and subsidiary facilities is determined for a range of five to 500 pounds of TNT. A correlation is established between the total cost and the charge weight designed for these facilities.